Meccanica (2020) 55:1499–1507
https://doi.org/10.1007/s11012-020-01185-3

Newtonian plane Couette flow with dynamic wall slip

M. S. Abou-Dina · M. A. Helal · Ahmed F. Ghaleb · George Kaoullas · Georgios C. Georgiou

Received: 12 December 2019 / Accepted: 22 May 2020 / Published online: 8 June 2020

Abstract The occurrence of slip complicates the estimation of the viscosity in rheometric flows. Thus, special analyses and experimental protocols are needed in order to obtain reliable estimates of the viscosity and other rheological parameters. In the present work, the plane Couette flow of a Newtonian fluid is considered allowing the possibility of dynamic wall slip, i.e. slip with a slip-relaxation parameter, along the fixed plate. For comparison purposes, the analytical solution corresponding to static slip, i.e. to the Navier slip condition, is derived first. Then, the dynamic-slip solution is obtained using separation of variables as well as the one-sided Fourier transform method. Both methods give essentially the same results. The effects of the slip and slip-relaxation parameters on the solution are discussed. It is demonstrated that flow dynamics becomes slower in the presence of slip and decelerates further as the value of the slip-relaxation parameter is increased.

Keywords Plane Couette flow · Start-up flow · Newtonian fluid · Navier slip · Dynamic slip · Fourier transform

M. S. Abou-Dina · M. A. Helal · A. F. Ghaleb
Department of Mathematics, Faculty of Science, Cairo University, Giza 12613, Egypt

G. Kaoullas · G. C. Georgiou (✉)
Department of Mathematics and Statistics, University of Cyprus, P.O. Box 20537, 1678 Nicosia, Cyprus
e-mail: georgios@ucy.ac.cy

1 Introduction

The role of wall slip in various processes of industrial importance, e.g. in polymer processing and in microfluidics, has been emphasized in recent reviews. Hatzikiriakos [1, 2] and Malkin and Patlazhan [3] reviewed wall slip of polymer melts and complex fluids, while Neto et al. [4] reviewed experimental studies of wall slip exhibited by Newtonian liquids. The occurrence of slip has also been observed in nanoscale experiments [5] and in molecular dynamic simulations of Newtonian [6] and non-Newtonian flows [7].

The most common slip equation is Navier's slip law [8], which relates the wall shear stress, σ_w^*, to the slip velocity, v_s^*, defined as the velocity of the fluid relative to that of the wall:

$$v_s^* = \frac{\sigma_w^*}{\beta^*} \tag{1}$$

where β^* is the slip coefficient, which is in general a function of temperature, normal stress and pressure, and the characteristics of the fluid/wall interface [9]. It should be noted that throughout the paper dimensional quantities and variables are denoted by stars. The no-slip boundary condition is recovered from Eq. (1) when $\beta^* \to \infty$. In many experimental studies on various fluid systems, it has been observed that wall slip occurs only above a certain critical value of the wall shear stress, known as the slip yield stress ([10]

and references therein). A number of nonlinear slip laws have also been proposed, the most popular of which is the power-law one:

$$v_s^* = \frac{\sigma_w^{*m}}{\beta^*} \tag{2}$$

where m is the exponent.

Equations (1) and (2) are static in the sense that the slip velocity adjusts instantaneously to the wall shear stress. Pearson and Petrie [11] were the first to propose a generic slip equation with relaxation time (i.e., memory) in which the slip velocity also depends on the past states of the wall shear stress:

$$v_s^* + \lambda_s^* \frac{dv_s^*}{dt^*} \equiv f(\sigma_w^*) \tag{3}$$

where λ_s^* is the slip relaxation time. The simplest form of the above equation is:

$$v_s^* + \lambda_s^* \frac{dv_s^*}{dt^*} \equiv \frac{\sigma_w^*}{\beta^*} \tag{4}$$

For steady slip flow the second term of the LHS of Eq. (4) is zero and Eq. (1) is recovered. Based on experimental observations on the stick–slip instability of polymer melts, in an attempt to describe the transition from the slip to the stick condition which exhibits characteristics of a relaxation process, Hatzikiriakos and Dealy [12] extended Eq. (4) to

$$v_s^* + \lambda_s^* \frac{dv_s^*}{dt^*} \equiv \frac{\sigma_w^{*m}}{\beta^*}, \tag{5}$$

studied the validity of the latter equation, and estimated the value of λ_s^* by observing slip in a transient flow. The reader is referred to Ref. [13] for a comprehensive review of early works where Eqs. (4) and (5) have been used. Interestingly, the molecular dynamics simulations carried out by Thalakkottor and Mohseni [14] for gas and simple liquid flows near a wall revealed that wall slip follows Eq. (4). Kaoullas and Georgiou [13] derived analytical solutions of the plane and axisymmetric Poiseuille flows and of the plane circular Couette flows with dynamic slip at all the walls following Eq. (4). More recently, Ebrahimi et al. [15] carried out steady and dynamic shear experiments on a polymer melt (HDPE) using a rotational rheometer and employed an integral viscoelastic constitutive equation to predict the transient shear response under no slip, static slip, and dynamic slip following Eq. (5). They reported two values for the stress relaxation time (for walls of different properties), i.e. $\lambda_s^* = 0.107$ s and $\lambda_s^* = 0.224$ s.

The plane Couette flow, also known as simple shear flow, is very important in rheology. The fluid sample is placed between two parallel flat plates and flow is generated by the rectilinear motion of one plate relative to the other so that the plates remain parallel and the distance between them is constant with time. A number of rheometers are based on this flow, e.g. the sliding plate rheometer [16], which is useful for constructing material functions in both steady and unsteady settings. The flow was used in the molecular dynamics simulations of Thompson and Troian [6] for a Newtonian fluid, which revealed the existence of a general nonlinear slip law. It has also been a benchmark for hydrodynamic stability studies [17]. Pedrossian et al. [17] have recently reviewed works on the stability of the flow at high Reynolds numbers.

The analysis of rheometric data becomes more complicated in the presence of slip [2]. Roughened walls are used in most cases in order to suppress slip. Another option is to attach sand paper to the shearing geometries. As pointed out by Coussot [18], the selection of the correct roughness may not be straightforward depending on the material under study.

Georgiou [19] solved numerically and investigated the stability of the time-dependent plane shear flow of an Oldroyd-B fluid with nonlinear static slip along the fixed wall. Ferrás et al. [20] also solved the steady-state plane Couette flow for generalized Newtonian fluids assuming that slip occurs only along the fixed plate and using both linear (Navier) and nonlinear static slip laws. Philippou et al. [21] solved analytically both the plane and circular Couette flows of a Newtonian fluid, using a linear slip law with a non-zero threshold slip stress and derived both the steady-state and the cessation solutions.

The objective of the present work is to derive analytical solutions of plane Couette flow with dynamic wall slip. To simplify the analysis, we consider here Eq. (4), which is linear. As in the previous works of Georgiou [19] and by Ferrás et al. [20], it is assumed that slip occurs only along the fixed plate. Suppressing slip along one or both walls is common practice in rheometry. For example, Piau and Piau [22] investigated the plane Couette flow of

viscoplastic materials, where one wall moves at constant speed and the other one vibrates, assuming that slip occurs only at the latter wall. Davies and Stokes [23] used a rotational parallel plate rheometer to study the rheology of Carbopol solutions using a roughened plate to suppress slip effects. In their circular-Couette rheological measurements, Ahuja and Singh [24] first used serrated cup and rotor in order to eliminate slip and then allowed slip along the motor by means of a wax coating.

The governing equations are presented and dedimensionalised in Sect. 2, where the steady-state solution is also provided. Two are the dimensionless numbers describing the flow, the slip number and the slip-relaxation number, which involve β^* and λ_s^*, respectively. In Sect. 3, the time-dependent solution is derived using both the separation of variables and the one-sided Fourier transform methods. The results for the special case of Navier slip (zero slip-relaxation number) are also provided and discussed in order to facilitate the subsequent discussion, In Sect. 4, after providing realistic ranges of the slip and slip-relaxation numbers. Deduced from the experiments of Ebrahimi et al. [15], we discuss the effects of these two parameters on the evolution of the solution. Finally, some concluding remarks are provided in Sect. 5.

2 Governing equations and steady-state solution

We consider the flow of a Newtonian fluid contained between infinite, horizontal parallel plates, placed at a distance H^* apart. The fluid is assumed to be at rest and suddenly the upper plate starts moving horizontally at a speed V^* while the lower one is kept fixed, as shown in Fig. 1.

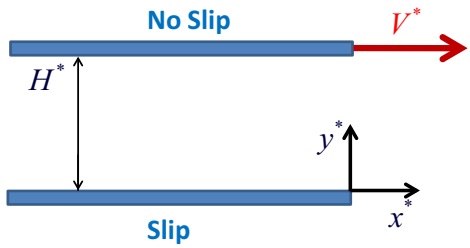

Fig. 1 Geometry of simple shear flow

Assuming that the flow is unidirectional and that gravity is negligible, the x-component of the momentum equation is reduced to

$$\frac{\partial v^*}{\partial t^*} = \nu^* \frac{\partial^2 v^*}{\partial y^{*2}} \tag{6}$$

where $v^* = v^*(y^*, t^*)$ is the velocity in the x-direction and ν^* is the kinematic viscosity. The latter is defined by $\nu^* \equiv \eta^*/\rho^*$, where η^* is the viscosity and ρ^* is the density of the fluid. It is assumed that no-slip occurs at the upper plate, while at the lower plate dynamic slip occurs following Eq. (4). Given that

$$\sigma_w^* = \eta^* \frac{\partial v^*(0, t^*)}{\partial y^*} \tag{7}$$

the boundary conditions for this initial boundary value problem read:

$$v^*(0, t^*) + \lambda_s^* \frac{\partial v^*(0, t^*)}{\partial t^*} = \frac{\eta^*}{\beta^*} \frac{\partial v^*(0, t^*)}{\partial y^*}, \quad t^* \geq 0 \tag{8}$$

and

$$v^*(H^*, t^*) = V^*, \quad t^* > 0 \tag{9}$$

The initial condition is given by

$$v^*(y^*, 0) = 0, \quad 0 \leq y^* \leq H^* \tag{10}$$

It is more convenient to dedimensionalize the problem of Eqs. (6)–(10). To this end we scale the velocity by V^*, lengths by H^*, and time by $H^{*2}/(\nu^* V^*)$:

$$v \equiv \frac{v^*}{V^*}, \quad y \equiv \frac{y^*}{H^*}, \quad t \equiv \frac{t^*}{H^{*2}/(\nu^* V^*)} \tag{11}$$

With the above scalings, the problem is dedimenionalized as follows:

$$\frac{\partial v}{\partial t} = \frac{\partial^2 v}{\partial y^2} \tag{12}$$

$$v(0, t) + \Lambda_s \frac{\partial v(0, t)}{\partial t} = \frac{1}{B} \frac{\partial v(0, t)}{\partial y}, \quad t \geq 0 \tag{13}$$

$$v(1, t) = 1, \quad t > 0 \tag{14}$$

$$v(y, 0) = 0, \quad 0 \leq y \leq 1 \tag{15}$$

where

$$\Lambda_s \equiv \frac{\lambda_s^* V^*}{H^*} \tag{16}$$

and

$$B \equiv \frac{\beta^* H^*}{\eta^*} \tag{17}$$

are the dimensionless slip-relaxation and slip numbers, respectively.

The steady-state solution $\bar{v} = \bar{v}(y)$ is easily obtained by solving the problem:

$$\frac{d^2\bar{v}}{dy^2} = 0, \quad \bar{v}(0) = \frac{1}{B}\frac{d\bar{v}(0)}{\partial y}, \quad \bar{v}(1) = 1 \tag{18}$$

It should be noted that in steady-state the dynamic slip term in the boundary condition vanishes, and the steady-state solution is the same as that corresponding to Navier slip. Solving the problem (18) yields:

$$\bar{v}(y) = \frac{By + 1}{B + 1} \tag{19}$$

The no-slip solution $\bar{v}(y) = y$ is recovered when $B \to \infty$. As for the steady-state slip velocity, this is given by

$$\bar{v}_s = \bar{v}(0) = \frac{1}{B + 1} \tag{20}$$

and, thus, it vanishes when $B \to \infty$.

3 Time-dependent solutions

Two methods of solution have been used in order to derive the solution of problem (12)–(15), the standard separation of variables (Fourier) method and the one-sided Fourier method. As discussed below, the two solutions are equivalent despite their different forms.

3.1 Solution by separation of variables

When dynamic wall slip is considered, the solution of Eq. (12) subject to (13)–(15) may be easily obtained by separation of variables in the form:

$$v(y,t) = \frac{By + 1}{B + 1} - 2\sum_{k=1}^{\infty} \frac{\sin[\alpha_k(1-y)]}{\alpha_k\left[1 + \frac{\cos^2\alpha_k}{B(1-\Lambda_s\alpha_k^2)} + 2B\Lambda_s\sin^2\alpha_k\right]} e^{-\alpha_k^2 t} \tag{21}$$

where the eigenvalues α_k are the roots of

$$\tan\alpha_k + \frac{\alpha_k}{B(1 - \Lambda_s\alpha_k^2)} = 0, \quad k = 1, 2, \ldots \tag{22}$$

Since the eigenvalues a_k appear in the boundary condition (13) special care must be taken when considering the (non-standard) orthogonality relation of the resulting Sturm–Liouville problem. The interested reader is referred to Ref. [13] for details. For the sake of calculation of the eigenvalues a_k, one verifies the following:

(1) If $0 < \Lambda^{-1/2} \le \frac{\pi}{2}$ then $k\pi < \alpha_k < \left(k + \frac{1}{2}\right)\pi$, $k = 1, 2, \ldots$.

(2) If $\left(n - \frac{1}{2}\right)\pi < \Lambda^{-1/2} \le \left(n + \frac{1}{2}\right)\pi, \quad n = 1, 2, \ldots,$ then

$$\begin{cases} (k - 1/2)\pi < \alpha_k < k\pi, & k = 1, 2, \ldots, n \\ k\pi < \alpha_k < (k + 1/2)\pi, & k = n + 1, n + 2, \ldots \end{cases}$$

The slip velocity is given by

$$v_s(t) = v(0,t) = \frac{1}{B+1} - 2\sum_{k=1}^{\infty} \frac{\sin\alpha_k}{\alpha_k\left[1 + \frac{\cos^2\alpha_k}{B(1-\Lambda_s\alpha_k^2)} + 2B\Lambda_s\sin^2\alpha_k\right]} e^{-\alpha_k^2 t} \tag{23}$$

In the case of static (Navier) slip, i.e. when $\Lambda_s = 0$, the velocity is given by

$$v(y,t) = \frac{By + 1}{B + 1} - 2\sum_{k=1}^{\infty} \frac{\sin[\alpha_k(1-y)]}{\alpha_k\left(1 + \frac{\cos^2\alpha_k}{B}\right)} e^{-\alpha_k^2 t} \tag{24}$$

where the eigenvalues α_k are the roots of

$$\tan\alpha_k + \frac{\alpha_k}{B} = 0, \quad k = 1, 2, \ldots \tag{25}$$

The slip velocity is simplified as follows:

$$v_s(t) = v(0,t) = \frac{1}{B+1} - 2\sum_{k=1}^{\infty} \frac{\sin\alpha_k}{\alpha_k\left(1 + \frac{\cos^2\alpha_k}{B}\right)} e^{-\alpha_k^2 t} \tag{26}$$

The classical no-slip solution [25] is recovered as the limiting case when $B \to \infty$:

$$v(y,t) = y - 2\sum_{k=1}^{\infty} \frac{1}{\alpha_k}\sin[\alpha_k(1-y)]e^{-\alpha_k^2 t} \tag{27}$$

where now $\alpha_k = k\pi, \quad k = 1, 2, \ldots$.

Figure 2 illustrates the evolution of the velocity to the corresponding steady-state solution for three slip numbers, i.e. for $B = \infty$ (no slip), 10 (moderate slip) and 1 (strong slip). It can be observed that the differences are more pronounced close to the lower wall where slip occurs. Moreover, we note that slip decelerates the convergence of the time-dependent solution to the steady-state, an effect that has also been observed in other theoretical [13] and experimental [26] works. This is also illustrated in Fig. 3, where the evolution of the slip velocity is plotted for different values of the slip numbers; as slip is enhanced, i.e. as B is reduced, the convergence to the steady-state value becomes slower.

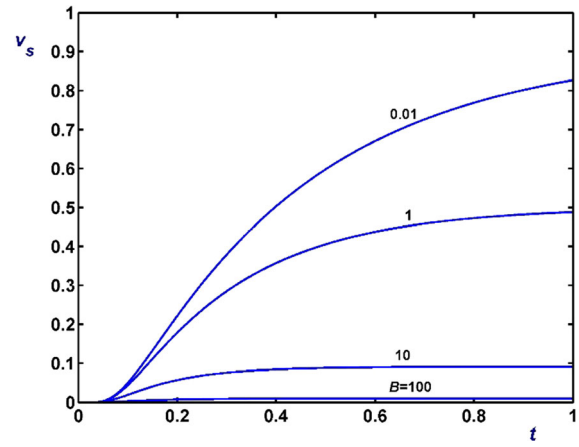

Fig. 3 Evolution of the slip velocity in the case of Navier slip ($\Lambda_s = 0$) for different slip numbers

3.2 Solution by one-sided Fourier transform

We present here an alternative method of solution, based on the one-sided Fourier transform. This technique is convenient to deal with more general boundary conditions on the slip boundary, in cases for which the separation of variables may not be adequate.

In what concerns infinite integrals which we intend to use in the sequel, it is known that absolute convergence of the integrand yields convergence of the infinite integral [27]. If the function is bounded and, moreover, tends to zero fast enough, then convergence of the infinite integral is guaranteed. This condition is not satisfied in the problem under consideration, in view of the boundary condition at the upper plate. To remedy this situation, and anticipating its boundedness, the dependent variable is transformed as follows:

$$v(y,t) = w(y,t)\, e^{At}, \tag{28}$$

where A is a positive parameter. The choice of an exponential damping factor is convenient for numerical considerations. At the end of the solution process, this parameter will be taken arbitrarily small and $w(y,t)$ will converge to the solution $v(y,t)$. Function $w(y,t)$ decays exponentially and the existence of the infinite integral of this function may now be easily verified:

$$\left|\int_0^\infty w(y,t)e^{i\xi t}dt\right| = \left|\int_0^\infty v(y,t)e^{-At}e^{i\xi t}dt\right| \leq M\int_0^\infty e^{-At}dt = \frac{M}{A} \tag{29}$$

where M is the upper bound of $|v(y,t)|$.

The transformed problem in terms of the new dependent variable $w(y,t)$ reads:

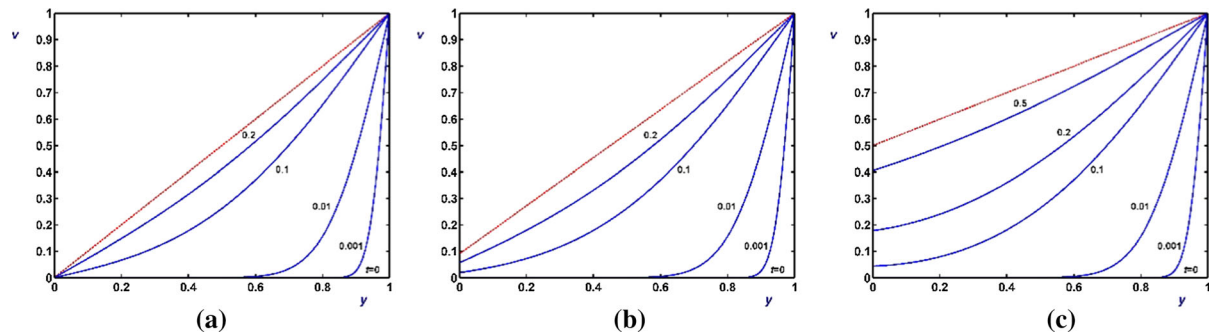

Fig. 2 Evolution of the velocity in the case of Navier slip ($\Lambda_s = 0$) for different slip numbers: **a** $B = \infty$ (no slip); **b** $B = 10$ (moderate slip); **c** $B = 1$ (strong slip). The straight line is the asymptotic steady-state solution

$$\frac{\partial w}{\partial t} + Aw = \frac{\partial^2 w}{\partial y^2} \tag{30}$$

$$w(0,t) + \Lambda_s \left[Aw(0,t) + \frac{\partial w(0,t)}{\partial t} \right] = \frac{1}{B} \frac{\partial w(0,t)}{\partial y}, \quad t \geq 0 \tag{31}$$

$$w(1,t) = e^{-At}, \quad t > 0 \tag{32}$$

$$w(y,0) = 0, \quad 0 \leq y \leq 1 \tag{33}$$

Now define the one-sided Fourier transform of $w(y,t)$ by means of:

$$\tilde{w}(y,\xi) = \int_0^\infty w(y,t)\, e^{i\xi t} dt \tag{34}$$

This formula readily shows that the complex conjugate of the function $\tilde{w}(y,t)$ is simply obtained by changing the sign of the variable ξ inside the integral. To the authors' knowledge, such a transform was seldom considered in the available literature, although it is quite useful in tackling certain initial-boundary-value problems. Taking the initial condition into account, it is straightforward to show that the transform $\tilde{w}(y,t)$ satisfies the second-order differential equation

$$\frac{\partial^2 \tilde{w}(y,\xi)}{\partial y^2} - (A - i\xi)\tilde{w}(y,\xi) = 0 \tag{35}$$

with boundary conditions

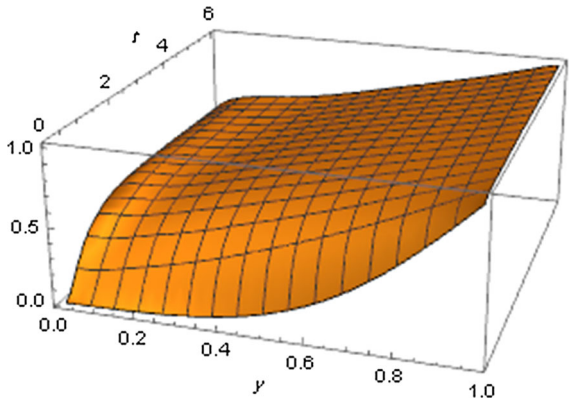

Fig. 4 Solution $v(y,t)$ for $\Lambda_s = 1$ and $B = 1$ (strong slip)

$$[1 + \Lambda_s(A - i\xi)]\tilde{w}(0,\xi) = \frac{1}{B} \frac{\partial \tilde{w}(0,\xi)}{\partial y}, \tag{36}$$

$$\tilde{w}(1,\xi) = \frac{1}{A - i\xi}. \tag{37}$$

The solution of Eq. (35) satisfying boundary conditions (36) and (37) is easily seen to be:

$$\tilde{w}(y,\xi) = C_1(\xi) e^{\alpha(\xi) y} + C_2(\xi) e^{-\alpha(\xi) y} \tag{38}$$

where

$$\alpha(\xi) = \sqrt{A - i\xi} \tag{39}$$

The coefficients C_1 and C_2 are determined by solving the following linear system:

$$\left.\begin{aligned} \left[1 + \Lambda_s(A - i\xi) - \frac{\alpha(\xi)}{B}\right] C_1 + \left[1 + \Lambda_s(A - i\xi) + \frac{\alpha(\xi)}{B}\right] C_2 = 0 \\ e^{\alpha(\xi)} C_1 + e^{-\alpha(\xi)} C_2 = \frac{1}{A - i\xi} \end{aligned}\right\} \tag{40}$$

Having determined the Fourier transform $\tilde{w}$, we may confine ourselves to its real part only, then perform the inverse Fourier cosine transform to obtain the function $w(y,t)$ from the rule:

$$w(y,t) = \frac{2}{\pi} \int_0^\infty \mathrm{Re}[\tilde{w}(y,\xi)] \cos(\xi t) d\xi. \tag{41}$$

Hence, the required solution to the initial problem is:

$$v(y,t) = w(y,t) e^{At}. \tag{42}$$

where the calculated solutions have to be improved by repeating the calculation for smaller values of A until convergence is achieved.

Comparisons of the two solutions derived here have shown that these are equivalent and indistinguishable. The results presented hereafter have all been obtained with separation of variables.

4 Results

Before showing representative results, it is important to know the order of the two dimensionless parameters in real experiments. For this purpose, we use values reported recently by Ebrahimi et al. [15] who carried out experiments with polydisperse linear polymers using partitioned plate and reported measurements of

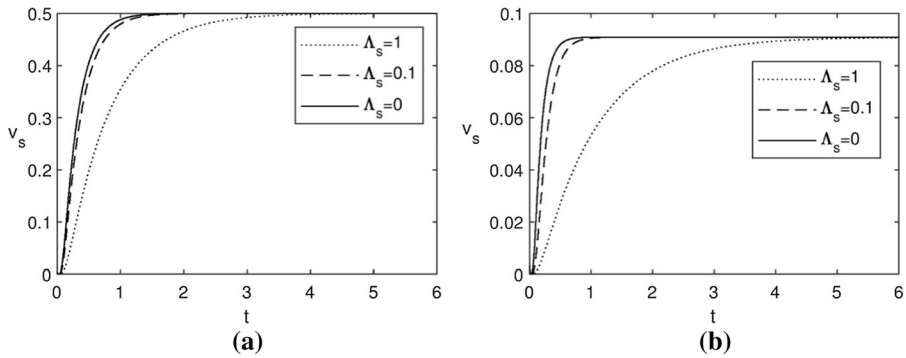

Fig. 5 Slip velocity $v(0,t)$ for various values of the slip-relaxation number Λ_s: **a** $B = 1$ (strong slip); **b** $B = 10$ (moderate slip). The solid lines correspond to Navier slip ($\Lambda_s = 0$)

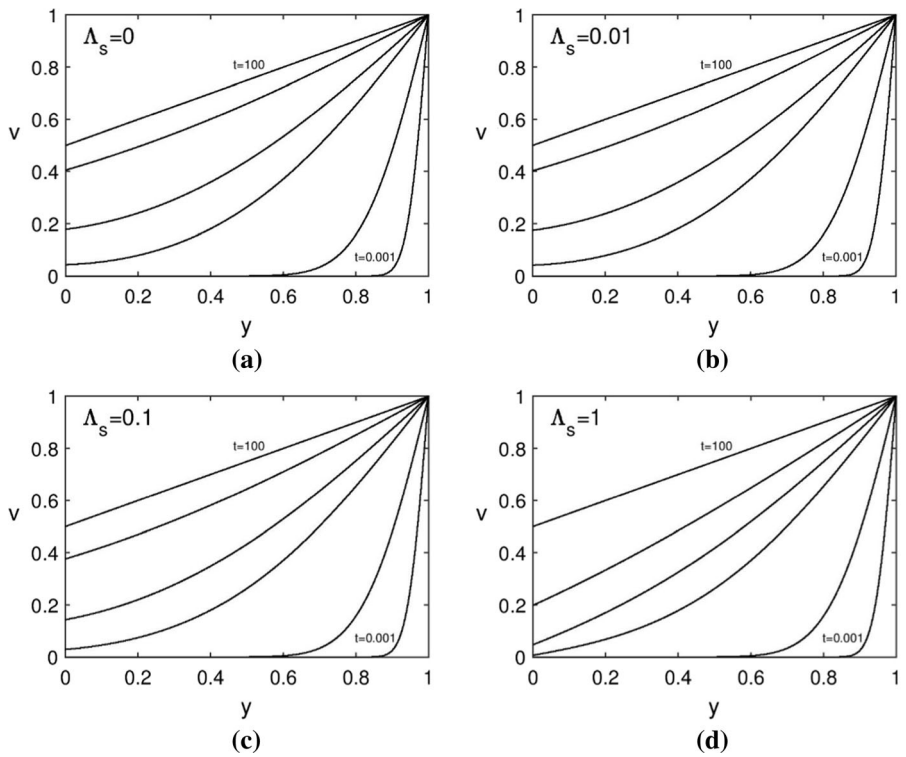

Fig. 6 Evolution of the velocity profile for $B = 1$ (strong slip) and various values of the slip-relaxation number: **a** $\Lambda_s = 0$; **b** $\Lambda_s = 0.01$; **c** $\Lambda_s = 0.1$; **d** $\Lambda_s = 1$. The profiles at $t = 0.001$, 0.01, 0.2, 0.5 and 100 (practically the steady-state solution) are shown

dynamic slip obeying slip Eq. (4). These authors experimented with three gaps, i.e. $H^* = 0.5,\ 0.75,\ 1$ mm, and reported two values for the slip relaxation time, i.e. $\lambda_s^* = 0.107,\ 0.224$ s. A representative estimate of the (steady-state) slip coefficient β^* was deduced from Fig. 7 of their paper observing that $\sigma_w^* = 0.1$ MPa when $v_s = 2$ mm/s: $\beta^* = \sigma_w^*/v_s^* = 5 \cdot 10^7$ Kg/m^2/s. For the speed of the upper plate, we assume that this ranges from $V^* = 2$ mm/s, i.e. the slip velocity used above to calculate the slip coefficient, up to 20 mm/s. Since Ebrahimi et al. [15] studied viscoelastic fluids, a representative viscosity should be considered. At a stress of 0.1 MPa, the viscosity value can be $\eta^* = 10^4$ Pa s. More specifically, the stress of 0.1 MPa corresponds to a frequency of about 10/s,

as it is easily deduced from Fig. 1 of Ebrahimi et al. [15] (the stress is equal to the frequency times the viscosity). Taking all the above into account, it turns out that B is in the range 2.5–5 and Λ_s in the range 0.214–8.96.

The solution $v(y,t)$ is illustrated in Fig. 4 for $\Lambda_s = 1$, $B = 1$ and times in the range 0–6. This is bounded, has a nearly constant slope and tends to a non-zero steady-state as time grows to infinity. Figure 5 shows the slip velocity as function of time for $B = 1$ (strong slip) and $B = 10$ (moderate slip), respectively, and three values of the slip-relaxation number. An expected saturation behavior is noticed as time grows larger, with saturation level independent of parameter Λ_s, but strongly dependent on B. The damping effect of these two parameters is obvious. An increase of Λ_s retards reaching the steady-state.

Figures 6 and 7 illustrate the evolution with time of the velocity profile for $B = 1$ (strong slip) $B = 10$ (moderate slip), respectively, and four values of the slip-relaxation number Λ_s (including $\Lambda_s = 0$, which corresponds to Navier slip). It is clear that for a given value of B, the steady-solution, which is independent of the slip-relaxation parameter, is reached. As expected, both parameters decelerate the evolution of the solution to this state.

As stated above, the results obtained by the one-sided Fourier transform were essentially the same as those of the separation-of-variables method. The integration over the infinite interval was approximated by an integration over the interval $[0, 20]$. As to the artificial parameter A, it was allowed to run over values in the interval $[0.0001, 0.01]$, the corresponding solutions were all identical as expected. For higher values of this parameter, however, oscillations of the solutions on Fig. 5 started to be noticed for large time values. These oscillations grew larger as A was augmented. It is our belief that these oscillations are due to the arising rounding errors, which at the end are amplified by the exponential factor in the R.H.S. of Eq. (28).

5 Conclusions

The start-up Newtonian Couette flow with dynamic slip along the fixed wall has been solved analytically

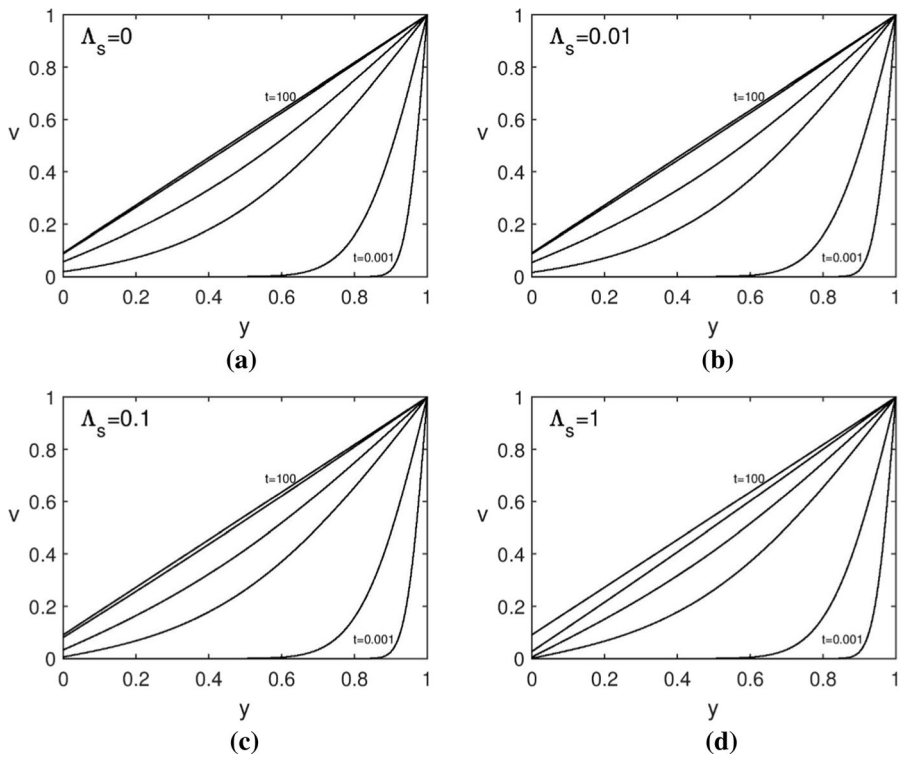

Fig. 7 Evolution of the velocity profile for $B = 10$ (moderate slip) and various values of the slip-relaxation number: **a** $\Lambda_s = 0$; **b** $\Lambda_s = 0.01$; **c** $\Lambda_s = 0.1$; **d** $\Lambda_s = 1$. The profiles at $t = 0.001$, 0.01, 0.2, 0.5 and 100 (practically the steady-state solution) are shown

using the separation of variables and the one-sided Fourier transform methods. The two methods yield equivalent results. The effects of the slip and slip-relaxation parameters have been discussed and representative ranges of the two parameters corresponding to certain experiments were deduced. It is demonstrated that both parameters have a damping effect on the evolution of the time-dependent solution.

The fact that reaching a steady state in the presence of dynamic wall slip may take very long times is of importance in rheometry. The analytical solution presented here may be useful in calculating the slip relaxation coefficients from transient experiments on both Newtonian and generalized-Newtonian (e.g. power-law) fluids. More systematic experimental data on both Newtonian and non-Newtonian fluids will be most useful in understanding better the implications of dynamic slip in practice.

Acknowledgements GCG acknowledges useful discussions with Professor Savvas G. Hatzikiriakos, University of British Columbia, Canada.

Compliance with ethical standards

Conflict of interest The authors declare that they have no conflict of interest.

References

1. Hatzikiriakos SG (2012) Wall slip of molten polymers. Prog Polym Sci 37:624–643
2. Hatzikiriakos SG (2015) Slip mechanisms in complex fluid flows. Soft Matter 11:7851–7856
3. Malkin AY, Patlazhan SA (2018) Wall slip for complex fluids—phenomenon and its causes. Adv Colloid Interface Sci 257:42–57
4. Neto C, Evans DR, Bonaccurso E, Butt HJ, Craig VSJ (2005) Boundary slip in Newtonian liquids: a review of experimental studies. Rep Prog Phys 68:2859–2897
5. Bonaccurso E, Kappl M, Butt HJ (2002) Hydrodynamic force measurement: boundary slip of water on hydrophilic surfaces and electrokinetic effects. Phys Rev Lett 88:076103
6. Thompson PA, Troian SM (1997) A general boundary condition for liquid flow at solid surfaces. Nature 389:360–362
7. Jabbarzadeh A, Atkinson JD, Tanner RI (1999) Wall slip in the molecular dynamics simulation of thin films of hexadecane. J Chem Phys 111:2612–2620
8. Navier CLMH (1827) Sur les lois du mouvement des fluids. Mem Acad R Sci l'Inst Fr 6:389–440
9. Denn MM (2001) Extrusion instabilities and wall slip. Annu Rev Fluid Mech 33:265–287
10. Damianou Y, Georgiou GC, Moulitsas I (2013) Combined effects of compressibility and slip in flows of a Herchel–Bulkley fluid. J Non Newton Fluid Mech 193:89–102
11. Pearson JRA, Petrie CJS (1968) On melt flow instability of extruded polymers. In: Wetton RE, Whorlow RW (eds) Polymer systems: deformation and flow. McMillan, London, pp 163–187
12. Hatzikiriakos SG, Dealy JM (1991) Wall slip of molten high density polyethylene. I. Sliding plate rheometer studies. J Rheol 35:497–523
13. Kaoullas G, Georgiou GC (2015) Start-up Newtonian Poiseuille and Couette flows with dynamic wall slip. Meccanica 50:1747–1760
14. Thalakkottor JJ, Mohseni K (2013) Analysis of boundary slip in a flow with an oscillating wall. Phys Rev E 87:03318
15. Ebrahimi M, Konaganti VK, Hatzikiriakos SG (2018) Dynamic slip of polydisperse linear polymers using partitioned plate. Phys Fluids 30:030601
16. Dealy JM, Wang J (2013) Melt rheology and its applications in the plastics industry, 1ns edn. Springer, Dordrecht
17. Pedrossian J, Germain P, Masmoudi N (2019) Stability of the Couette flow at high Reynolds numbers in two and three dimensions. Bull Am Math Soc 56:373–414
18. Coussot PJ (2005) Rheometry of pasted suspensions and granular materials: applications in industry and environment. Wiley, New York
19. Georgiou GC (1996) On the stability of the shear flow of a viscoelastic fluid with slip along the fixed wall. Rheol Acta 35:39–47
20. Ferrás LL, Nóbrega JM, Pinho FT (2012) Analytical solutions for Newtonian and inelastic non-Newtonian flows with wall slip. J Non Newton Fluid Mech 175–176:76–88
21. Philippou M, Damianou Y, Miscouridou X, Georgiou GC (2017) Cessation of Newtonian circular and plane Couette flows with wall slip and non-zero slip yield stress. Meccanica 52:2081–2099
22. Piau M, Piau JM (2005) Plane Couette flow of viscoplastic materials along a slippery vibrating wall. J Non Newton Fluid Mech 125:71–85
23. Davies GA, Stokes JR (2008) Thin film and high shear rheology of multiphase complex fluids. J Non Newton Fluid Mech 148:73–87
24. Ahuja A, Singh A (2009) Slip velocity of concentrated suspensions in Couette flow. J Rheol 53:1461–1485
25. Papanastasiou T, Georgiou G, Alexandrou A (1999) Viscous fluid flow. CRC Press, Boca Raton
26. Poumaere A, Moyers-Gonzalez M, Castelain C, Burghelea T (2014) Unsteady laminar flows of a carbopol gel in the presence of wall slip. J Non Newton Fluid Mech 205:28–40
27. Titchmarsh EC (1939) The theory of functions, 2nd edn. Oxford University Press, Oxford